In Vivo Misfolding of Proinsulin Below the Threshold of Frank Diabetes

Israel Hodish, Afaf Absood, Leanza Liu, Ming Liu, Leena Haataja, Dennis Larkin, Ahmed Al-Khafaji, Anthony Zaki, and Peter Arvan

OBJECTIVE—Endoplasmic reticulum (ER) stress has been described in pancreatic β-cells after onset of diabetes—a situation in which failing β-cells have exhausted available compensatory mechanisms. Herein we have compared two mouse models expressing equally small amounts of transgenic proinsulin in pancreatic β-cells.

RESEARCH DESIGN AND METHODS—In hProCpepGFP mice, human proinsulin (tagged with green fluorescent protein [GFP] within the connecting [C]-peptide) is folded in the ER, exported, converted to human insulin, and secreted. In hProC(A7)Y-CpepGFP mice, misfolding of transgenic mutant proinsulin causes its retention in the ER. Analysis of neonatal pancreas in both transgenic animals shows each β-cell stained positively for endogenous insulin and transgenic protein.

RESULTS—At this transgene expression level, most male hProC(A7)Y-CpepGFP mice do not develop frank diabetes, yet the misfolded proinsulin perturbs insulin production from endogenous proinsulin and activates ER stress response. In nondiabetic adult hProC(A7)Y-CpepGFP males, all β-cells continue to abundantly express transgene mRNA. Remarkably, however, a subset of β-cells in each islet becomes largely devoid of endogenous insulin, with some of these cells accumulating large quantities of misfolded mutant proinsulin, whereas another subset of β-cells has much less accumulated misfolded mutant proinsulin, with some of these cells containing abundant endogenous insulin.

CONCLUSIONS—The results indicate a source of pancreatic compensation before the development of diabetes caused by proinsulin misfolding with ER stress, i.e., the existence of an important subset of β-cells with relatively limited accumulation of misfolded proinsulin protein and maintenance of endogenous insulin production. Generation and maintenance of such a subset of β-cells may have implications in the avoidance of type 2 diabetes. ***Diabetes*** **60:2092–2101, 2011**

During early type 2 diabetes, morphological abnormalities have been identified within the secretory pathway of pancreatic islet β-cells. Specifically, the endoplasmic reticulum (ER) and pre-Golgi intermediates become distended (herein called ER crowding), and some β-cells develop a deficiency of secretory granules (1,2). Similar morphological features have also been reported in various monogenic forms of diabetes that may develop an "impacted-ER phenotype" (3,4). As best we can tell, morphological ER crowding is correlated with ER stress, as evidenced by activation of ER stress response signaling pathways. Morphological ER crowding is not critical in simple overfeeding (3), suggesting that ER crowding may be a specific link to β-cell dysfunction. However, most research demonstrating ER crowding/ER stress in pancreatic β-cells has focused on models that are already hyperglycemic at the time of study. Once hyperglycemia commences, additional metabolic insults (a process known as glucotoxicity [5–7]) may cause further β-cell injury. Although one can anticipate that some degree of ER crowding/ER stress may exist even before deterioration of glycemic control, this process is less well studied.

Mutant *INS* gene–induced diabetes of youth (MIDY) (8) is a syndrome with an established genetic basis (9), caused by preproinsulin-coding sequence mutations that trigger misfolding, which leads to autosomal-dominant, insulin–deficient diabetes. The same disease occurs also in *Akita* (10) and Munich (11) mice. Secondary defects in proinsulin folding may also occur as a consequence of alterations in the proinsulin folding environment in the ER (4,12). Hyperglycemia may exacerbate such an unfavorable environment, creating a potential linkage between proinsulin misfolding in the ER and type 2 diabetes (13–15). Before the onset of overt hyperglycemia, we have our best chance to identify early pancreatic compensatory responses that may help to limit diabetes progression.

In this study, we have characterized a mouse model expressing exclusively in pancreatic β-cells a transgene containing the same proinsulin-C(A7)Y mutation as that found in *Akita* mice (16). It is noteworthy that the folding-defective proinsulin known as "hProC(A7)Y-CpepGFP" (bearing green fluorescent protein [GFP] within the connecting [C]-peptide) is expressed at subthreshold levels, such that very few mice develop frank diabetes in the absence of additional metabolic or genetic insult. These animals can be studied side by side with transgenic mice that exhibit comparable β-cell–specific expression of hProCpepGFP lacking any misfolding-inducing mutation (17). The presence of the GFP tag itself does not prevent proinsulin folding, trafficking, processing, or secretion (17) but allows for detection and localization of the protein in β-cells. The present studies highlight pathways of islet compensation in the setting of underlying proinsulin misfolding, which may have relevance for understanding early type 2 diabetes.

RESEARCH DESIGN AND METHODS

Materials. Rabbit antisera against GFP was from Immunology Consultants (Newberg, OR); anti–α-tubulin was from Santa Cruz Biotechnology (Santa Cruz, CA); anti-immunoglobulin heavy chain-binding protein (BiP) was from Cell Signaling (Danvers, MA); AlexaFluor-488–conjugated anti-GFP was from Invitrogen (Carlsbad, CA); peroxidase-conjugated anti-rabbit and peroxidase-conjugated anti–guinea pig were from Jackson ImmunoResearch Laboratories

From the Division of Metabolism, Endocrinology, and Diabetes, University of Michigan Medical Center, Ann Arbor, Michigan.
Corresponding authors: Israel Hodish, ihodish@umich.edu; Peter Arvan, parvan@umich.edu.
Received 1 December 2010 and accepted 17 May 2011.
DOI: 10.2337/db10-1671

(West Grove, PA); AlexaFluor-555–conjugated anti-rabbit was from Invitrogen; rat insulin radioimmunoassay (RIA) was from Millipore (Billerica, MA); mouse proinsulin ELISA was from ALPCO (Salem NH); and collagenase-P and proteinase inhibitor mixture were from Roche Applied Science (Indianapolis, IN).

Construction of the hProCpepGFP and hProC(A7)Y-CpepGFP transgenes. The emerald GFP cDNA was inserted into the C-peptide–coding sequence within the human insulin cDNA to create hProCpepGFP (17). The hProC(A7)Y-CpepGFP then used PCR mutagenesis to replace Cys(A7) with Tyr in the coding sequence. *XhoI*-flanking restriction sites were used to insert these constructs downstream of the 8.3-kb mouse *Ins1* promoter and upstream of the nontranslated human growth hormone gene (18).

Generation of transgenic mice. The linearized hProC(A7)Y-CpepGFP transgene was injected into pronuclei of fertilized mouse eggs at the University of Michigan Transgenic Animal Model Core. PCR genotyping was performed by PCR with GFP-specific primers (forward primer, 5′-AGG TCT ATA TCA CCG CCG ACA-3′; reverse primer, 5′-TGC AGT AGT TCT CCA GCT GGT AG-3′), yielding a 400-bp product. One line (of 10) was propagated, housed in a pathogen-free facility, and fed standard rodent chow in accordance with the University of Michigan Animal Care Committee. Unless otherwise stated, all experiments were done with 3–6-month-old nondiabetic male mice (e.g., Figs. 1*A*, 4*A*, 5, and 8). Intraperitoneal glucose tolerance tests were performed on fasted animals with 1.0 mg dextrose per gram body weight. For some experiments, hProCpepGFP and hProC(A7)Y-CpepGFP mice were mated to *Ins2*$^{-/-}$ mice (from C. Polychronakos, McGill University, Montreal, Quebec, Canada) to increase the ratio between the products of transgenic and endogenous *Ins1* alleles. In other experiments, compound heterozygotes bearing both wild-type hProCpepGFP and *Akita* mutant proinsulin were used as a control for the hProC(A7)Y-CpepGFP line that carries both elements in a single allele.

Immunofluorescence. Fixed pancreata (formaldehyde plus 10% sucrose) were snap-frozen; 7-μm sections were permeabilized in acetone, blocked, and immunolabeled with guinea pig anti-insulin or antiglucagon and secondary antibodies in PBS containing 0.5% BSA. For BiP and GFP, de-paraffinized sections were heated in citrate (pH 5.0), cooled, blocked, incubated overnight with anti-BiP and appropriate secondary, blocked again, incubated overnight with AlexaFluor-488–conjugated anti-GFP, and mounted for confocal microscopy.

Pancreatic islet isolation. Pancreata were digested in 2 mg/mL collagenase-P for 30 min at 37°C, washed, and handpicked and incubated in RPMI 1640 medium containing either 4 or 16.7 mmol/L glucose (plus 10% fetal bovine serum and 1% penicillin–streptomycin) for 48 h.

Western blotting. Islet proteins were resolved by 4–12% gradient SDS-PAGE under reducing conditions; electrotransferred to nitrocellulose; probed with anti-insulin, anti-GFP, and anti–α-tubulin (loading control); and probed with appropriate peroxidase-conjugated secondary antibodies for enhanced chemiluminescence.

Real-time PCR. cDNA from template mRNA (RNeasy; QIAGEN, Valencia, CA) was generated by reverse transcriptase (SuperScript III; Invitrogen) and amplified with *Taq* polymerase in a real-time thermal cycler (denaturation 30 s, annealing 30 s, and extension 3 min) using appropriate primers, and SYBR green fluorescence followed each cycle. The following primers were used:

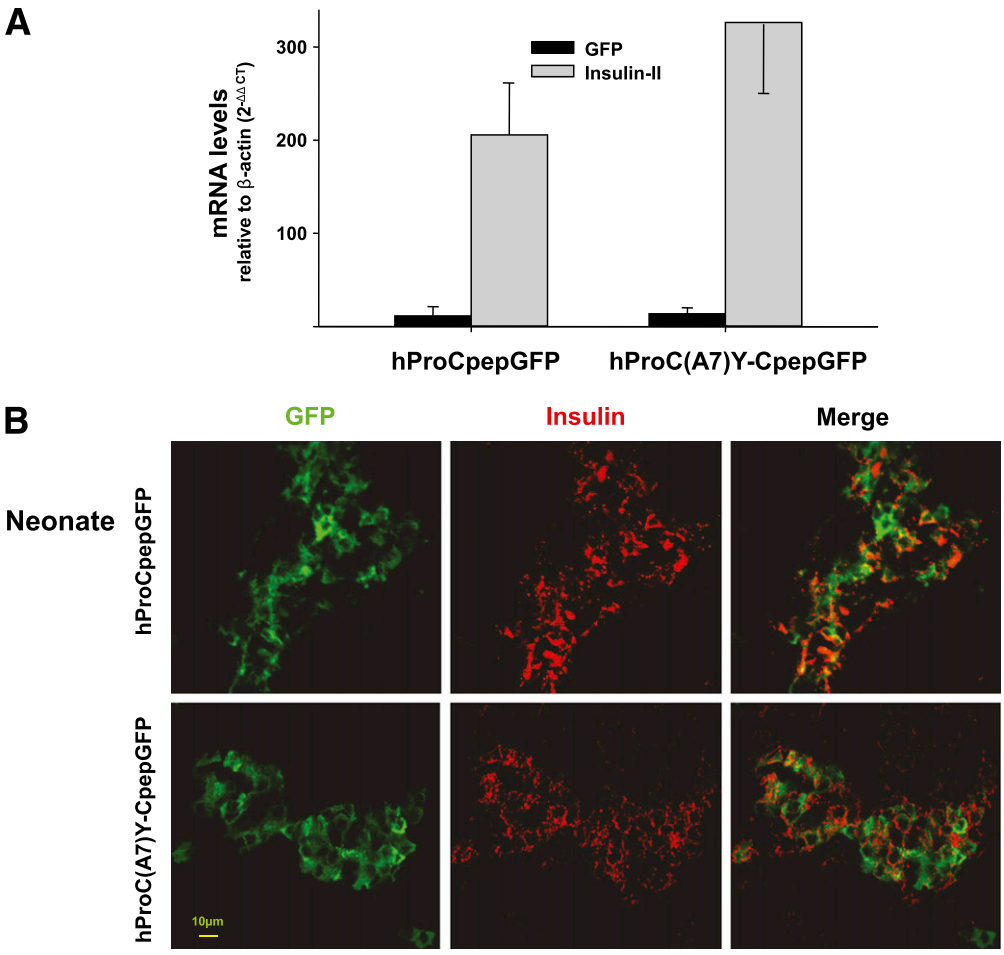

FIG. 1. Endogenous proinsulin and transgenic GFP-labeled proinsulin. ***A*****: mRNA levels from islets from three to four hProCpepGFP and hProC(A7)Y-CpepGFP mice. Islet mRNA extraction was followed by synthesis of reverse-transcribed cDNAs; specific primers for endogenous preproinsulin-II and GFP were then used to measure mRNA abundance relative to β-actin mRNA, as quantified by real-time PCR ($2^{-\Delta\Delta CT}$ ± SEM). The ratio of transgene mRNA to endogenous preproinsulin-II mRNA is similar in the islets of hProCpepGFP (5.5%) and hProC(A7)Y-CpepGFP transgenic mice (4.2%); in both cases, >95% of insulin mRNA is derived from endogenous genes.** ***B*****: Distribution of endogenous and GFP-labeled insulin + proinsulin among the β-cells of neonatal males. Neonatal pancreatic tissue was snap frozen in liquid nitrogen and 7-μm sections were analyzed. GFP epifluorescence identified transgenic proinsulin and its derived products, while endogenous proinsulin-derived products were immunolabeled with anti-insulin antibodies. Scale bars are identical for each image shown. Even in hProC(A7)Y-CpepGFP males, most neonatal β-cells mutually express both endogenous insulin and GFP-labeled mutant proinsulin. (A high-quality digital representation of this figure is available in the online issue.)**

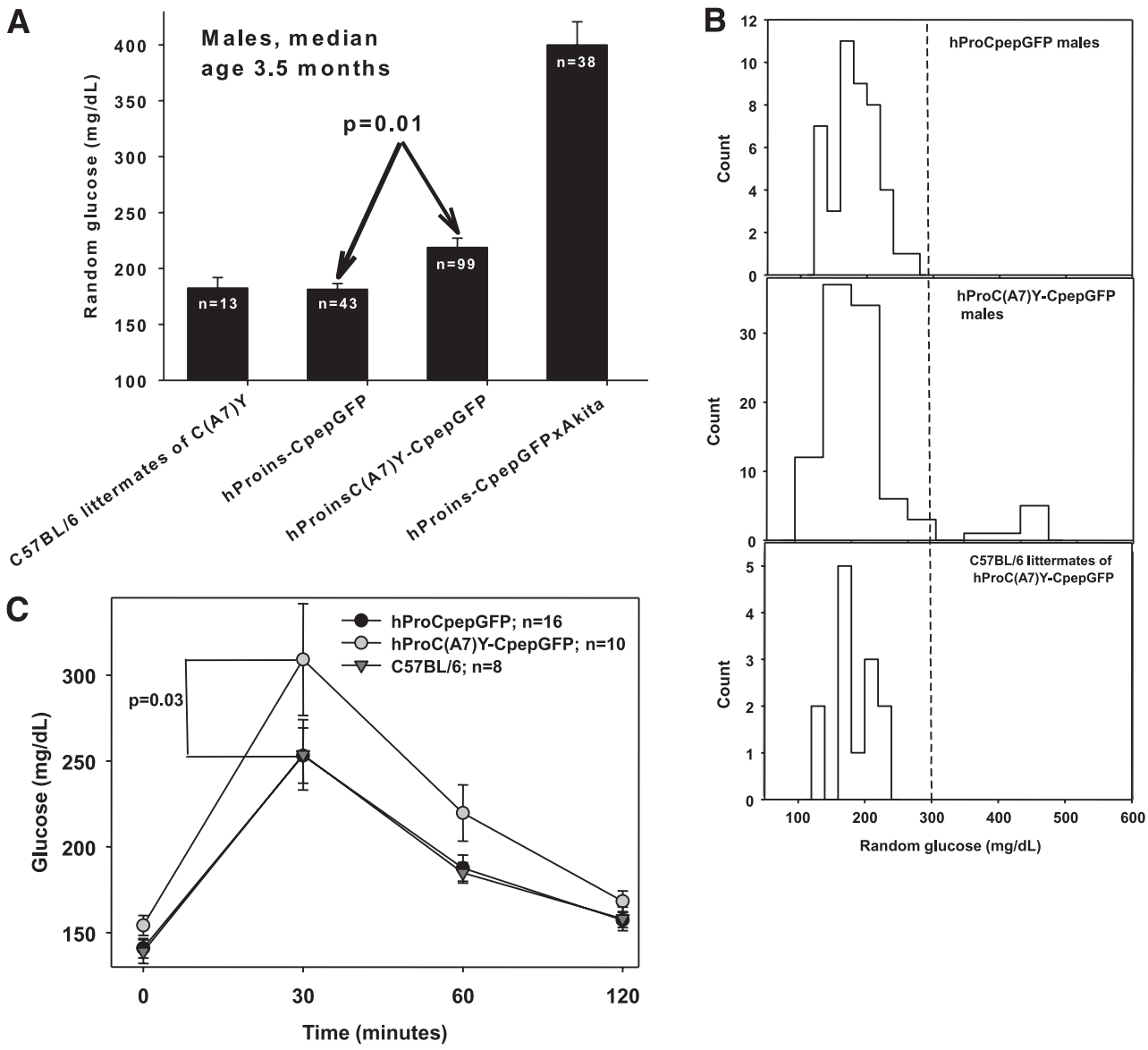

FIG. 2. Blood glucose levels in male mice (median age 3.5 months). *A*: Random blood glucose was obtained by tail snip from males of the different genotypes indicated. Mean random glucose of hProC(A7)Y-CpepGFP transgenic males was significantly higher than that of hProCpepGFP transgenic males, but less than that of hProCpepGFP transgenic males bearing one endogenous Ins2 *Akita* allele (bar at right). *B*: Histograms of random blood glucose measurements of individual male mice; each animal is shown only once. (Retesting of the small proportion [~10%] of hProC (A7)Y-CpepGFP animals with random blood glucose exceeding 300 mg/dL reconfirmed diabetes in these animals.) *C*: Intraperitoneal glucose tolerance tests (1 mg dextrose/g body weight) were performed on fasted animals. Compared with hProCpepGFP and C57BL/6 control mice, the results confirm that the hProC(A7)Y-CpepGFP males have impaired glucose tolerance.

GFP, 5′-AGG TCT ATA TCA CCG CCG ACA-3′ and 5′-TGC AGT AGT TCT CCA GCT GGT AG-3′; preproinsulin-II, 5′-CCC TGC TGG CCC TGC TCT T-3′ and 5′-AGG TCT GAA GGT CAC CTG CT-3′; BiP, 5′-GGC CAA ATT TGA AGA GCT GA-3′ and 5′-GCT CCT TGC CAT TGA AGA AC-3′; CHOP, 5′- CAT ACA CCA CCA CAC CTG AAA G-3′ and 5′-CCG TTT CCT AGT TCT TCC TTG C-3′; XBP-1, 5′-TGG CCG GGT CTG CTG AGT CCG-3′ and 5′-GTC CAT GGG AAG ATG TTC TGG-3′; spliced XBP-1, 5′-CTG AGT CCG AAT CAG GTG CAG-3′ and 5′-GTC CAT GGG AAG ATG TTC TGG-3′; and β-actin, 5′-TAT TGG CAA CGA GCG GTT CC-3′ and 5′-GGC ATA GAG GTC TTT ACG GAT GTC-3′. mRNA levels (normalized to β-actin) were calculated using the comparative threshold cycle (CT) method ($2^{-\Delta\Delta CT}$).

In situ hybridization. A 175-bp, digoxigenin–labeled oligonucleotide probe complementary to GFP mRNA was used for in situ hybridization with anti–digoxigenin-phosphatase detection as described elsewhere (19). As a negative control, pancreatic islets from C57BL/6 mice were negative for detectable mRNA.

Image analysis. For each genotype, epifluorescence images from twenty 0.5-cm diameter pancreatic (tail) cryosections from three mice, with identical exposures, were quantified in grayscale using Adobe Photoshop CS3. To identify the predominant (pro)insulin (GFP-labeled or endogenous) in each β-cell, a sensitivity threshold was established at midrange of the pixel intensity histogram for each section. Cellular areas with signals above threshold for each type of (pro)insulin were demarcated, and DAPI staining identified each nucleus. Of the total cellular area of fluorescence, cells containing >80% GFP fluorescence area were classified as cells expressing primarily GFP-labeled proinsulin; cells expressing >80% insulin immunofluorescence area were classified as cells expressing primarily endogenous insulin; and β-cells expressing both in which neither label predominated were classified as expressing both. Cell boundaries (not shown) were corroborated by immunolabeling with anti–β-catenin.

Quantification was performed using NIH ImageJ 1.37c software. Results presented are mean ± SEM. Statistical analyses were performed using one-way ANOVA with Tukey multiple comparisons; $P \leq 0.05$ was considered significant.

Transmission electron microscopy. Pancreatic tissue from nondiabetic hProC(A7)Y-CpepGFP mice was fixed in buffered glutaraldehyde, postfixed in OsO_4, dehydrated with graded alcohols and propylene oxide, embedded in

Spurr's resin, and sectioned at 70 nm, grids-stained with uranyl acetate and lead citrate, and examined on a Philips CM-100 electron microscope.

RESULTS

Transgene expression in hProCpepGFP and hProC(A7)Y-CpepGFP mice. Two transgenic lines were used. The hProCpepGFP mouse carries a GFP-labeled proinsulin (17), whereas the hProC(A7)Y-CpepGFP mouse carries a similar GFP-labeled proinsulin bearing the misfolding-inducing *Akita* mutation. In islets isolated from the two mouse lines, we examined an abundance of mRNAs encoding these GFP-labeled preproinsulins and the endogenous *Ins2* mRNA levels (*Ins2* represents the majority of total insulin transcripts in mouse islets [20]). Using qPCR (normalized to β-actin mRNA) with concentration standards of hProCpepGFP plasmid DNA, we confirmed that the levels of hProCpepGFP and hProC(A7)Y-CpepGFP mRNA represented only 5.5 and 4.2%, respectively, of that measured for endogenous *Ins2* mRNA (Fig. 1*A*).

We examined pancreatic cryosections from neonatal male hProCpepGFP and hProC(A7)Y-CpepGFP mice (sex determined by Y-chromosome PCR) using intrinsic GFP fluorescence and insulin immunofluorescence. At postnatal day 1, hProCpepGFP and hProC(A7)Y-CpepGFP male mice demonstrated GFP fluorescence (either properly folded or misfolded mutant proinsulin) in essentially all of the cells that were immunolabeled for endogenous insulin + proinsulin, i.e., in the vast majority of β-cells (Fig. 1*B*; quantified in Fig. 7*A*). Thus, the data in Fig. 1 indicate that the two animal models demonstrate comparable levels and patterns of transgene mRNA and protein expression across the β-cell population in vivo.

Most male hProC(A7)Y-CpepGFP transgenic mice avoid frank diabetes. We compared body weights and random glucose levels of hProC(A7)Y-CpepGFP transgenic mice with those of hProCpepGFP mice that are phenotypically identical to C57BL/6 littermates (17). Mean body weight of hProC(A7)Y-CpepGFP males was similar to that of normal control subjects, and mean random glucose of hProC(A7)Y-CpepGFP males (between 8:00 A.M. and 12:00 P.M.) was only modestly elevated and significantly lower than hProCpepGFP *Akita* males (Fig. 2*A*). A histogram of individual males of each genotype showed that random blood glucose levels in the vast majority (>85%) of hProC(A7)Y-CpepGFP males had a distribution largely overlapping with that of normal controls (Fig. 2*B*). Although a small subset of males (~10% of total) exhibited random hyperglycemia, the results indicate that the majority of animals with transgenic expression of hProC(A7)Y-CpepGFP (driven by the *Ins1* promoter) do not have frank diabetes (Figs. 2*A* and *B*), i.e., a considerably milder phenotype than *Akita* mice who bear the same mutation in one of the endogenous *Ins2* genes.

To identify subtler defects in islet performance in hProC(A7)Y-CpepGFP males, we subjected the animals to intraperitoneal glucose tolerance testing after an overnight fast. Although fasting glucose values were similar to those of hProCpepGFP and C57BL/6 control males, the hProC(A7)Y-CpepGFP males had a significantly higher mean blood glucose at 30 min poststimulation than control subjects (309 ± 32.6 vs. 253.1 ± 16.1 mg/dL; P = 0.03). Although a significant difference was not sustained at 120 min postchallenge, the results indicate that hProC(A7)Y-CpepGFP mice have impaired glucose tolerance (Fig. 2*C*).

Homozygous knockout of the endogenous *Ins2* gene (with homozygous expression of wild-type *Ins1* still remaining) itself does not cause diabetes (20). Therefore, we were interested to use homozygous *Ins2* knockout to examine the effect of increasing the relative expression of mutant hProC(A7)Y-CpepGFP (transgene) to wild-type insulin. In this background, mice with transgenic expression of wild-type hProCpepGFP were normoglycemic, whereas mice with transgenic expression of hProC(A7)Y-CpepGFP developed hyperglycemia that was particularly severe when both *Ins2* alleles were missing, including the cohort of female animals (Fig. 3, *bottom*). Thus, although the majority of mice exhibit sufficient compensation to accommodate low-level expression of misfolded proinsulin, these animals are nevertheless predisposed to diabetes, and the relative expression levels of misfolded and wild-type proinsulin dictate the phenotype (Fig. 3).

In nondiabetic hProC(A7)Y-CpepGFP mice, the production and maturation of endogenous proinsulin is perturbed by transgenic expression of misfolded mutant proinsulin. To determine whether pancreatic insulin content was comparable in nondiabetic hProC(A7)Y-CpepGFP transgenic mice and nonmutant control subjects, we measured total insulin + proinsulin (endogenous and transgenic) in isolated pancreatic islets. By RIA, islet insulin + proinsulin content per cell was significantly less than that measured for hProCpepGFP transgenic controls (Fig. 4*A*), despite that all islets were derived from nondiabetic animals. In the small subset of diabetic hProC(A7)

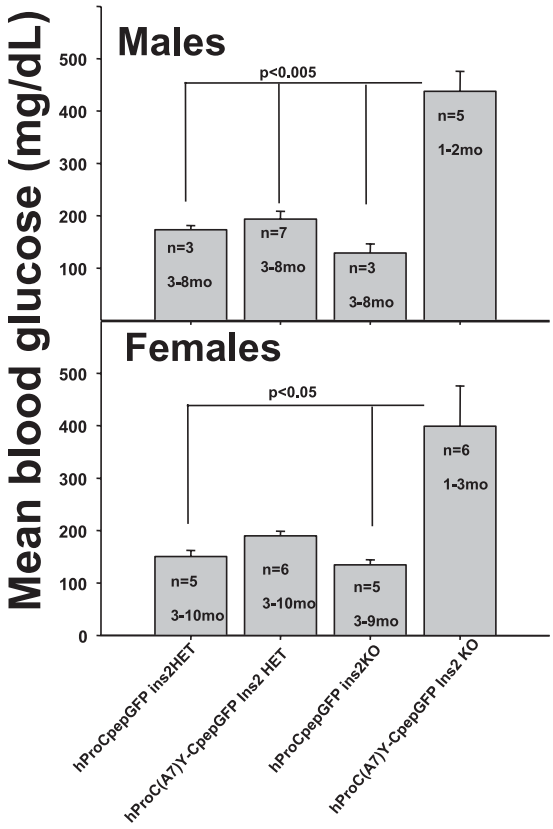

FIG. 3. Mean random glucose of transgenic male and female mice partially or completely devoid of endogenous Ins2. Transgenic mice were first mated with complete *Ins2* knockout animals to generate hProCpepGFP or hProC(A7)Y-CpepGFP, $Ins2^{+/-}$ animals (first two sets of bars) and then back bred to generate transgenic $Ins2^{-/-}$ animals (second two sets of bars). Results are depicted as mean ± SEM.

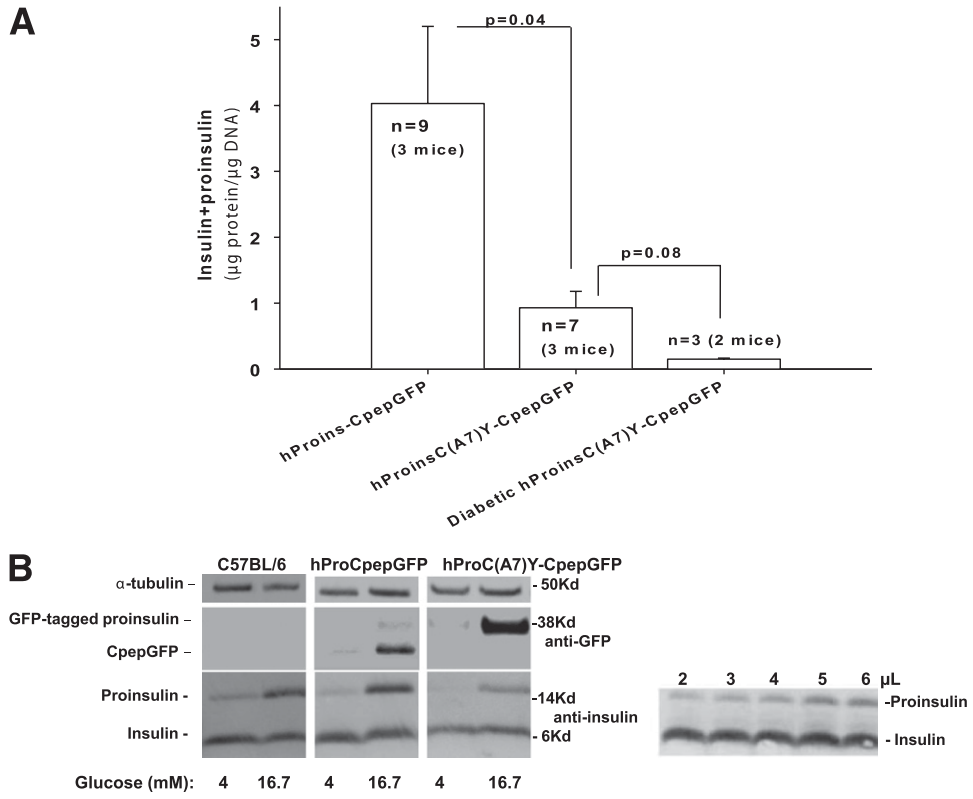

FIG. 4. Content of insulin and proinsulin and transgene-encoded products in mouse islets. *A*: Isolated islets from hProCpepGFP and hProC(A7)Y-CpepGFP transgenic males were lysed directly, and total insulin + proinsulin content measured by RIA. *B*: Isolated islets from hProCpepGFP and nondiabetic hProC(A7)Y-CpepGFP transgenic males were incubated in RPMI 1640 medium containing either 4 or 16.7 mmol/L glucose for 48 h before lysis. Islet lysates from three adult males of each genotype (plus C57BL/6 littermate controls) were pooled and analyzed by reducing SDS-PAGE and Western blotting with anti-insulin (*bottom*), anti-GFP (*middle*), and anti–α-tubulin (*top*). Note that endogenous proinsulin content is diminished in islets of nondiabetic hProC(A7)Y-CpepGFP mice. *Inset*: Different loading volumes of islet lysate from C57BL/6 mice indicate that Western blotting with anti-insulin appeared more sensitive to changes in proinsulin content than to changes in insulin, which may account for the relatively small change in appearance of the insulin band in islets of nondiabetic hProC(A7)Y-CpepGFP mice in *B* despite the larger apparent change in insulin + proinsulin content noted in *A*.

Y-CpepGFP males, the insulin + proinsulin content was lower still (<5% of control).

We also used an independent assay to follow proinsulin (and insulin) content in isolated islets incubated for 48 h in either 4 or 16.7 mmol/L glucose. Islet lysates were analyzed by reducing SDS-PAGE, electrotransferred to nitrocellulose, and immunoblotted with either anti-GFP (to follow the transgene product) or anti-insulin (to follow the endogenous product). In islets from both hProCpepGFP and hProC(A7)Y-CpepGFP mice, protein encoded by the transgene was up-regulated in response to incubation at high glucose. As expected, hProC(A7)Y-CpepGFP did not exhibit maturation, as measured by its inability to be endoproteolytically converted to CpepGFP, whereas hProCpepGFP was processed in secretory granules to CpepGFP (Fig. 4*B*). Endogenous proinsulin protein expression also was increased by high glucose; however, the amount of proinsulin was markedly less in islets of hProC(A7)Y-CpepGFP transgenic mice (Fig. 4*B*). The immunoblotted insulin band in islets of hProC(A7)Y-CpepGFP transgenic mice did not appear to be greatly affected by the high-glucose incubation; however, we found that when loading amounts that linearly report changes in proinsulin content (Fig. 4*B*, inset), insulin band-intensity changes were rather insensitive and may underestimate the insulin recovery defect in hProC(A7)Y-CpepGFP islets. Indeed by rodent proinsulin–specific RIA, we found that proinsulin content of the islets was 1.26% of total hormone content for both hProCpepGFP and C57BL/6 mice and 1.4% for nondiabetic hProC(A7)Y-CpepGFP mice. Altogether, the data of Fig. 4 suggest that the presence of misfolded mutant proinsulin decreases the levels of endogenous bystander proinsulin (Fig. 4*B*), concomitant with a decrease in islet insulin that occurs even in nondiabetic animals (Fig. 4*A*).

Islets of nondiabetic hProC(A7)Y-CpepGFP transgenic mice activate ER stress response. To determine whether expression of misfolded mutant hProC(A7)Y-CpepGFP below the diabetogenic threshold triggers ER stress response, mRNA levels for BiP and spliced XBP-1 were measured in freshly isolated islets from nondiabetic hProCpepGFP and hProC(A7)Y-CpepGFP transgenic mice. Indeed, islets of hProC(A7)Y-CpepGFP mice had significantly increased BiP mRNA, as well as a tendency to increased splicing of XBP-1 (Fig. 5). Furthermore, hProC(A7)Y-CpepGFP islets also exhibited a trend suggesting increased mRNA for CHOP (Fig. 5), a downstream component of the unfolded protein response pathway that predisposes to cell death (21–23). The results suggest that proinsulin misfolding by hProC(A7)Y-CpepGFP does induce ER stress, even in the absence of or before frank diabetes.

In hProC(A7)Y-CpepGFP transgenic mice, a subpopulation of β-cells in each islet exhibits misfolded proinsulin accumulation and poor endogenous insulin production. A recent report of PERK knockout mice has shown that a subpopulation of islet β-cells exhibits an "impacted-ER" phenotype characterized morphologically

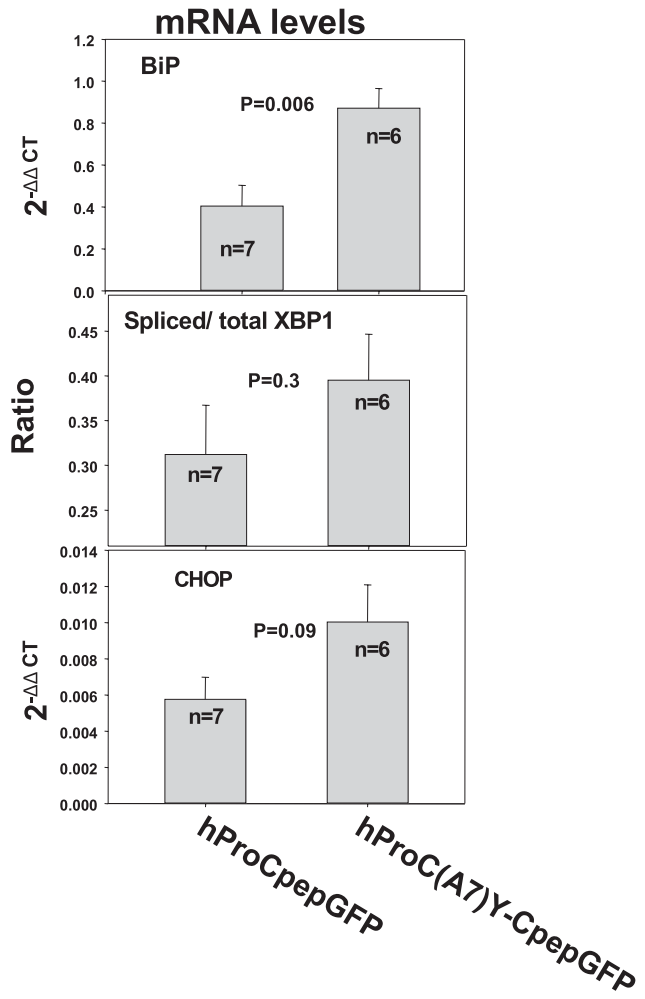

FIG. 5. ER stress response activation in islets of hProC(A7)Y-CpepGFP transgenic mice. Freshly isolated islets were extracted for RNA, followed by synthesis of reverse-transcribed cDNAs. Specific primers for BiP, spliced XBP1, total XBP1, and CHOP were used to quantify mRNA by real-time PCR, normalized to β-actin mRNA. Results are depicted as mean $2^{-\Delta\Delta CT}$ ± SEM. ER stress response is higher in islets of nondiabetic hProC(A7)Y-CpepGFP mice than in hProCpepGFP mice (which exhibit BiP, spliced/total XBP1, and CHOP mRNA levels that are not higher than those of C57BL/6 control islets).

by an expanded ER with accumulation of proinsulin (4), consistent with ER crowding (1,2). Because of the evidence of ER stress in islets of nondiabetic hProC(A7)Y-CpepGFP mice (Fig. 5), we looked for morphological correlates in the β-cells of these animals. In cryosections of adult male transgenic mice, hProCpepGFP or hProC (A7)Y-CpepGFP protein expression was detected by intrinsic GFP fluorescence, whereas anti-insulin immunostaining was used to reflect endogenous insulin protein.

As in neonatal males (Fig. 1*B*), islets of hProCpepGFP adult males (17) expressed the GFP-positive transgene product in virtually all β-cells, which were simultaneously positive for endogenous insulin (Fig. 6*A*; quantified in Fig. 7*B*). Remarkably, in contrast to neonatal animals, islets of nondiabetic hProC(A7)Y-CpepGFP males reproducibly exhibited heterogeneous β-cell subpopulations (Fig. 6*B*). Approximately 40% of the β-cells accumulated the fluorescent, misfolded mutant proinsulin, which, at higher magnification, exhibited an ER distribution pattern (Fig. 6*C*). Within each islet, β-cells rich in hProC(A7)Y-CpepGFP fluorescence tended to be largely devoid of insulin immunostaining; another major subpopulation of β-cells exhibited little GFP fluorescence and immunostained clearly for endogenous insulin; and only a small, third subpopulation accumulated both types of molecules (Fig. 7*B*).

To begin to understand the origin of the heterogeneity of hProC(A7)Y-CpepGFP accumulation within the β-cell population, we also examined hProC(A7)Y-CpepGFP mRNA distribution within the islets by in situ hybridization with a specific complementary oligonucleotide RNA probe. As exemplified in Fig. 6*D*, as much as 60% of transgene mRNA–positive β-cells within the population exhibited little or no hProC(A7)Y-CpepGFP fluorescence. Evidently, the other ~40% subpopulation of β-cells with misfolded proinsulin accumulation and little or no insulin immunostaining (Figs. 6*B* and 7*B*) develops during postnatal life. Even if the larger subpopulation of β-cells that failed to accumulate or had not yet accumulated significant quantities of misfolded proinsulin within the ER (Fig. 6*B*) contained all of the islet insulin that is recovered (Fig. 4*A*), the insulin content, even in this subpopulation of β-cells, must still be decreased compared with that of hProCpepGFP control islet β-cells.

As the islets of hProC(A7)Y-CpepGFP mice contained significantly increased BiP mRNA (Fig. 5), we also looked at the distribution of BiP protein compared with islets of hProCpepGFP mice. Although BiP was increased in many β-cells of hProC(A7)Y-CpepGFP mice, a heterogeneous pattern within the islets was observed (Fig. 8*A*, *left*). BiP tended to be increased in cells that had accumulated hProC(A7)Y-CpepGFP, but BiP was also increased in a few other cells that had not accumulated green fluorescence (Fig. 8*A*, *right*), suggesting that these cells also were synthesizing increased amounts of misfolded secretory protein.

To examine β-cell heterogeneity at the ultrastructural level, we performed transmission electron microscopy of the islets of nondiabetic hProC(A7)Y-CpepGFP islets. Populations of highly granulated β-cells were readily identified (Fig. 8*B*, β-cell #1). However, side by side with such cells were other β-cells with a highly expanded ER and many fewer (but definite) insulin secretory granules (Fig. 8*B*, β-cell #2). Upon close inspection, dilation of the ER was also seen in the β-cells that retained abundant insulin secretory granules (Fig. 8*C* and *D*, β-cell #1). β-Cells with a dramatically expanded ER compartment tended to have unusually small insulin secretory granule profiles (Fig. 8*C*, microgranules). Finally, we were also surprised to discover the unique morphological appearance of a third type of β-cell that also had insulin microgranules but lacked an expanded ER compartment; rather, such cells exhibited a highly shrunken cytoplasm (Fig. 8*D*, β-cells #2 and #3). It is not clear whether this third kind of β-cell has either sufficient hProC(A7)Y-CpepGFP protein or endogenous insulin protein to be detected either by GFP fluorescence or insulin immunofluorescence as was measured in Figs. 6 and 7.

Islets of nondiabetic hProC(A7)Y-CpepGFP mice are hyperplastic. To further clarify whether the decreased islet insulin is a consequence of a decrease of insulin within β-cells or a decrease in islet size and a resultant decrease of overall β-cell numbers, we examined multiple random pancreatic tail cryosections of 3–6-month-old nondiabetic hProCpepGFP and hProC(A7)Y-CpepGFP male mice. Islets contained within 0.2-cm^2 pancreatic cross-sections from three different mice of each genotype were identified, and, by use of GFP fluorescence plus immunostaining with anti-insulin, the islet boundaries were determined and the islet cell nuclei counted by DAPI staining. (Antiglucagon

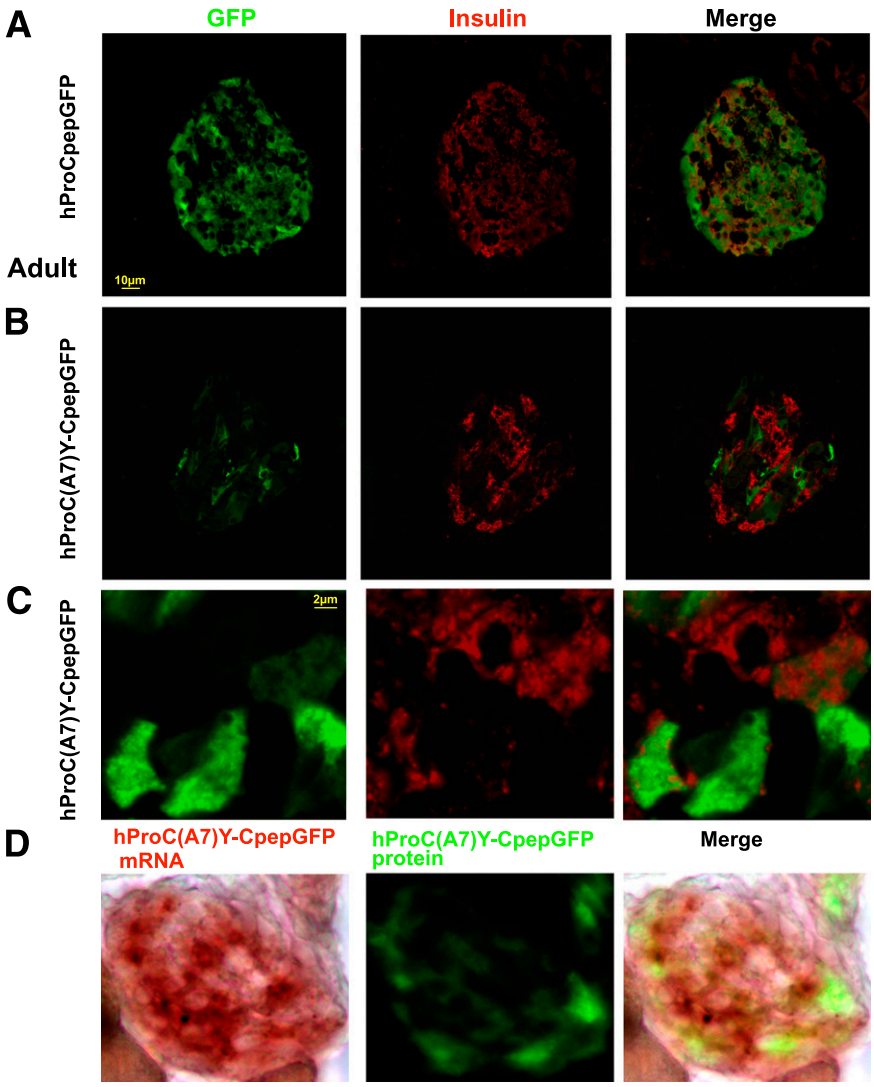

FIG. 6. Distribution of endogenous and GFP-labeled proinsulin + insulin among the cells within islets of adult males. *A*: Immunostaining with anti-insulin and GFP epifluorescence (performed as described in RESEARCH DESIGN AND METHODS) in an adult hProCpepGFP male. *B*: Nondiabetic hProC(A7)Y-CpepGFP adult male analyzed by identical methodology to that in *A*. *C*: A high magnification image showing the relative distribution of endogenous insulin and misfolded proinsulin in a population of β-cells from a transgenic hProC(A7)Y-CpepGFP adult male. *D*: Nondiabetic adult hProC(AY)Y-CpepGFP male analyzed by in situ hybridization to measure transgene-derived mRNA (*left*), transgene-derived protein assessed by epifluorescence (*middle*), and a superimposed image (*right*). Note that while all β-cells in the islet appear to contain transgene-derived hProC(A7)Y-CpepGFP mRNA, β-cells accumulating large quantities of GFP-labeled mutant proinsulin appear deficient of endogenous insulin + proinsulin. (A high-quality digital representation of this figure is available in the online issue.)

immunostaining was also performed in both sets of mice [not shown], confirming that α-cells did not exceed 10% of islet cells in either mouse line.)

On average, the random cross-sectional islet area of nonmutant hProCpepGFP mice (n = 21 islets) was 2,545 μm^2 (±276 SEM), similar to that obtained from C57BL/6 control mice (not shown), whereas random cross-sectional islet area of hProC(A7)Y-CpepGFP mice (n = 25 islets) averaged 4,221 μm^2 (±793 SEM), a considerable (65%) increase. On average, each hProCpepGFP islet cross-section contained 40.0 (±6.2 SEM) β-cell profiles, whereas each hProC(A7)Y-CpepGFP islet cross-section contained 62.8 (±23.7 SEM) β-cell profiles. Dividing average islet cross-sectional area by average number of β-cell profiles per cross-section, a rough estimate of average β-cell cross-sectional area was essentially unchanged between the two mouse lines. Thus, rather than β-cell hypertrophy, the data indicate an expansion of β-cell number per islet, suggesting β-cell hyperplasia in compensation for expression of misfolded proinsulin to help these animals avoid diabetes. Even when considering that many islet β-cells accumulating fluorescent misfolded mutant proinsulin have little or no endogenous insulin (Fig. 7*B*), there was not an actual loss of insulin-positive β-cells in nondiabetic hProC(A7)Y-CpepGFP islets, indicating that decreased islet insulin content in these animals (Fig. 4*A*) must be caused by a decrease of insulin content per β-cell.

DISCUSSION

Studies have suggested β-cell ER crowding/ER stress in animals in which hyperglycemia was already present (1,3,24). Glucotoxicity is a potentially confounding variable making other pathogenic mechanisms more difficult to analyze.

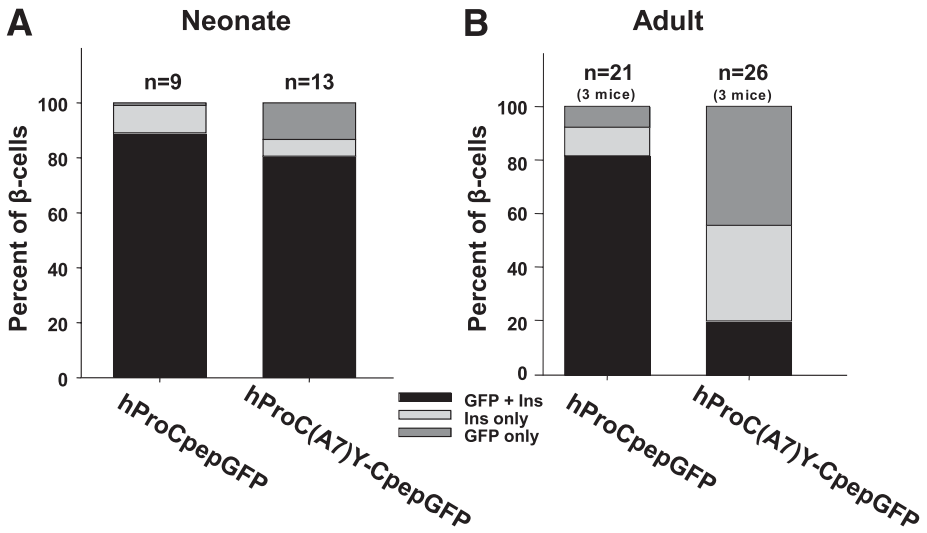

FIG. 7. Quantification of the distribution of endogenous and GFP-labeled proinsulin + insulin among the cells within islets of neonatal and adult transgenic male mice. Islet β-cells were scored for cells in which both endogenous and GFP-labeled proinsulin + insulin were detected (*black bars*), versus cells in which either endogenous insulin (*light gray*) or GFP-labeled proinsulin (*dark gray*) predominated. Cryosections of three adult and two neonatal mice of each group were used for quantification; *n* = number of islets examined. *A*: Percentage of cells accumulating each type of insulin + proinsulin in male neonates (sex determined by Y-chromosome PCR). *B*: Percentage of cells accumulating each type of insulin + proinsulin in nondiabetic adult males. Note that in hProC(A7)Y-CpepGFP adult males, only 20% of β-cells have accumulated protein derived from both endogenous and transgene-derived proinsulins.

Herein, we have compared nonmutant hProCpepGFP transgenic males to nondiabetic hProC(A7)Y-CpepGFP transgenic males, with each transgene accounting for only a few percent of proinsulin mRNA (Fig. 1). Whereas permanent neonatal diabetes occurs both in humans (9) and *Akita* males (10), the hProC(A7)Y-CpepGFP transgene is driven by the weak *Ins1* promoter coexpressed with four wild-type alleles; thus, diabetes penetrance is more subtle (Fig. 2). A distinct advantage of this model is that effects of frank diabetes are largely excluded, although hProC(A7)Y-CpepGFP males are rendered severely diabetic upon deletion of endogenous *Ins2*, i.e., when the relative expression of misfolded proinsulin to wild-type proinsulin is increased (Fig. 3). However, even in nondiabetic hProC(A7)Y-CpepGFP males with a full complement of endogenous *Ins* genes, islet β-cells have decreased insulin production (Fig. 4*A*), inhibited by coexpressed mutant proinsulin (Fig. 4*B*) as observed in β-cells of *Akita* males (17) (females tend to resist diabetes [25,26]).

In hProC(A7)Y-CpepGFP males, misfolded proinsulin and its dominant interference with endogenous proinsulin causes ER stress that increases BiP (Fig. 5), predating frank diabetes. Among other ER stress response targets, CHOP is proapoptotic (21–23). Nevertheless, the initial decrease of insulin production is not accompanied by decreased β-cell mass in *Akita* mice (4) or in prediabetic hProC(A7)Y-CpepGFP mice (this study). Evidently, either because of or in spite of ER stress responses, there is pancreatic compensation for proinsulin misfolding with decreased insulin production.

Surprisingly, we found that, in islets of nondiabetic adult hProC(A7)Y-CpepGFP transgenic males, despite that most or all β-cells express the transgene mRNA (Fig. 6*D*), misfolded proinsulin accumulation appears concentrated in a subpopulation of islet β-cells (Figs. 6*B* and 7*B*), as has recently been described in other mouse models (4). The fact that β-cell subpopulations are not detected on postnatal day 1 (Fig. 1*B*) suggests that β-cell heterogeneity develops during postnatal life. Preservation of insulin production includes maintenance of a robust pool of insulin secretory granules in a subpopulation (Figs. 6 and 8) that is undoubtedly linked to the islet compensation necessary to avoid diabetes. One hypothesis needing to be tested is that this might be explained by the slowly progressive appearance of new β-cells that have not yet accumulated the misfolded proinsulin product. Indeed, islets of nondiabetic hProC(A7)Y-CpepGFP male mice exhibit morphological evidence of β-cell hyperplasia within islets. Generation of new β-cells may be needed to compensate for others that have lost insulin production (generating only a few microgranules; Fig. 8*C* and *D*). Such a hypothesis interdigitates well with the fact that there are already known to be β-cell subpopulations in adult animals that operate at different rates of proinsulin biosynthesis (27–29), and this may include variability in secretory feedback on proinsulin synthesis (30) and secretion (31) as well as potentially different susceptibilities to cell stress (32). Of course, the mutant hProC(A7)Y-CpepGFP represents only a tiny fraction of total proinsulin mRNA (Fig. 1*A*) and an even smaller fraction of total β-cell protein synthesis. Thus, whether mutant proinsulin protein is variably synthesized among the different β-cells within islets (especially under different glucose conditions) is unknown.

It seems likely that there is a continuum of proinsulin misfolding, ER crowding, and ER stress in a range of diabetes subtypes, from permanent neonatal diabetes to type 2 diabetes. Unfortunately, not all genetically predisposed individuals exhibit sufficient compensatory responses to prevent diabetes. Our results are consistent with the suggestion that β-cell dysfunction exists before the onset of overt diabetes, and patients with such β-cell dysfunction may benefit from early pharmacological intervention to limit proinsulin misfolding or to preserve insulin production through suitable compensatory responses.

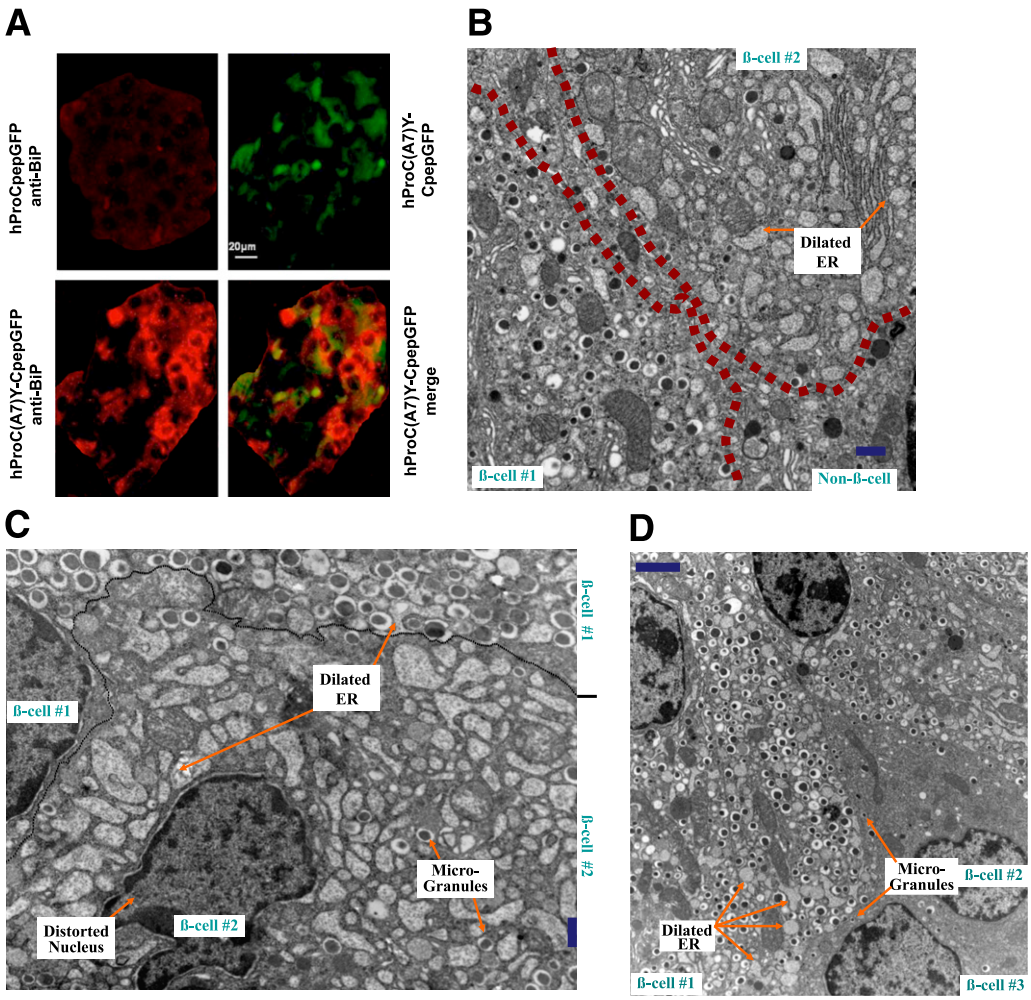

FIG. 8. BiP immunofluorescence and electron microscopic examination of the islets from hProC(A7)Y-CpepGFP transgenic mice. *A*: Four fluorescence images are shown; the top left represents islet immunofluorescence with anti-BiP in control hProCpepGFP mice. The remaining three panels are anti-GFP immunofluorescence, anti-BiP immunofluorescence, and merged fluorescence from hProC(A7)Y-CpepGFP transgenic mice. *B*: Electron micrograph from islet of nondiabetic male hProC(A7)Y-CpepGFP transgenic mouse. The cytoplasm of two β-cells and one non–β-cell is shown, revealing heterogeneity in the accumulation of insulin secretory granules (β-cell #1) and expansion of the ER compartment (β-cell #2). Plasma membranes are highlighted with a dashed line. Bar, 500 nm. *C*: Electron micrograph from islet of nondiabetic male hProC(A7)Y-CpepGFP transgenic mouse. The cytoplasm of two β-cells is shown, demonstrating that dilated ER is also present in β-cell #1 that is highly granulated. In β-cell #2, demonstrating expansion of the ER, rare insulin microgranules are detected. Plasma membranes are highlighted with a dashed line. Bar, 500 nm. *D*: Electron micrograph from islet of nondiabetic male hProC(A7)Y-CpepGFP transgenic mouse. The cytoplasm of three β-cells is shown, demonstrating that dilated ER is also present in β-cell #1 that is highly granulated. In β-cells #2 and #3, rare insulin microgranules are detected and dilation of the ER is not evident; moreover the entire β-cell cytoplasm is highly contracted. The boundaries between these cells are quite distinct so plasma membranes are not specifically highlighted. Bar, 2 μm. (A high-quality digital representation of this figure is available in the online issue.)

ACKNOWLEDGMENTS

This work was supported primarily by National Institutes of Health grants R00-DK-077441A (to I.H.) and R01-DK-48280 (to P.A.), a grant from the Michigan Diabetes Research and Training Center (to M.L.), and Endocrinology T32 grant (to L.L.).

No potential conflicts of interest relevant to this article were reported.

I.H. researched the data, contributed to the discussion, and wrote the manuscript. A.A., M.L., and L.H. researched the data and contributed to the discussion. L.L., D.L., A.A.-K., and A.Z. researched the data. P.A. contributed to the discussion, wrote the manuscript, and reviewed and edited the manuscript.

The authors acknowledge assistance from the University of Michigan Transgenic Mouse Core, Morphology and Image Analysis Core, Molecular Biology and DNA Sequencing Core, supported in part by P60-DK-20572, the University of Michigan Gut-Peptide Center, and the University of Michigan Cancer Center for assistance with electron microscopy. The authors thank Bill and Dee Brehm for improving diabetes research infrastructure at the University of Michigan.

REFERENCES

1. Like AA, Chick WL. Studies in the diabetic mutant mouse. II. Electron microscopy of pancreatic islets. Diabetologia 1970;6:216–242
2. Marchetti P, Bugliani M, Lupi R, et al. The endoplasmic reticulum in pancreatic beta cells of type 2 diabetes patients. Diabetologia 2007;50:2486–2494
3. Sachdeva MM, Claiborn KC, Khoo C, et al. Pdx1 (MODY4) regulates pancreatic beta cell susceptibility to ER stress. Proc Natl Acad Sci USA 2009; 106:19090–19095
4. Gupta S, McGrath B, Cavener DR. PERK (EIF2AK3) regulates proinsulin trafficking and quality control in the secretory pathway. Diabetes 2010;59: 1937–1947

5. Gerich JE. Is reduced first-phase insulin release the earliest detectable abnormality in individuals destined to develop type 2 diabetes? Diabetes 2002;51(Suppl. 1):S117–S121
6. Gopaul NK, Anggård EE, Mallet AI, Betteridge DJ, Wolff SP, Nourooz-Zadeh J. Plasma 8-epi-PGF2 alpha levels are elevated in individuals with non-insulin dependent diabetes mellitus. FEBS Lett 1995;368:225–229
7. Leahy JL, Bonner-Weir S, Weir GC. Minimal chronic hyperglycemia is a critical determinant of impaired insulin secretion after an incomplete pancreatectomy. J Clin Invest 1988;81:1407–1414
8. Liu MHI, Hodish I, Haataja L, et al. Proinsulin misfolding and diabetes: mutant INS gene-induced diabetes of youth. Trends Endocrinol Metab 2010;21:652–659
9. Støy J, Edghill EL, Flanagan SE, et al.; Neonatal Diabetes International Collaborative Group. Insulin gene mutations as a cause of permanent neonatal diabetes. Proc Natl Acad Sci USA 2007;104:15040–15044
10. Yoshioka M, Kayo T, Ikeda T, Koizumi A. A novel locus, Mody4, distal to D7Mit189 on chromosome 7 determines early-onset NIDDM in nonobese C57BL/6 (Akita) mutant mice. Diabetes 1997;46:887–894
11. Herbach N, Rathkolb B, Kemter E, et al. Dominant-negative effects of a novel mutated Ins2 allele causes early-onset diabetes and severe beta-cell loss in Munich Ins2C95S mutant mice. Diabetes 2007;56:1268–1276
12. Zito E, Chin KT, Blais J, Harding HP, Ron D. ERO1-beta, a pancreas-specific disulfide oxidase, promotes insulin biogenesis and glucose homeostasis. J Cell Biol 2010;188:821–832
13. Steiner DF, James DE. Cellular and molecular biology of the beta cell. Diabetologia 1992;35(Suppl. 2):S41–S48
14. Kirchhoff K, Machicao F, Haupt A, et al. Polymorphisms in the TCF7L2, CDKAL1 and SLC30A8 genes are associated with impaired proinsulin conversion. Diabetologia 2008;51:597–601
15. Loos RJ, Franks PW, Francis RW, et al. TCF7L2 polymorphisms modulate proinsulin levels and beta-cell function in a British Europid population. Diabetes 2007;56:1943–1947
16. Wang J, Takeuchi T, Tanaka S, et al. A mutation in the insulin 2 gene induces diabetes with severe pancreatic beta-cell dysfunction in the Mody mouse. J Clin Invest 1999;103:27–37
17. Hodish I, Liu M, Rajpal G, et al. Misfolded proinsulin affects bystander proinsulin in neonatal diabetes. J Biol Chem 2010;285:685–694
18. Hara M, Wang X, Kawamura T, et al. Transgenic mice with green fluorescent protein-labeled pancreatic beta-cells. Am J Physiol Endocrinol Metab 2003;284:E177–E183
19. Hitchcock P, Kakuk-Atkins L. The basic helix-loop-helix transcription factor neuroD is expressed in the rod lineage of the teleost retina. J Comp Neurol 2004;477:108–117
20. Leroux L, Desbois P, Lamotte L, et al. Compensatory responses in mice carrying a null mutation for Ins1 or Ins2. Diabetes 2001;50(Suppl. 1):S150–S153
21. Song B, Scheuner D, Ron D, Pennathur S, Kaufman RJ. Chop deletion reduces oxidative stress, improves beta cell function, and promotes cell survival in multiple mouse models of diabetes. J Clin Invest 2008;118:3378–3389
22. Oyadomari S, Koizumi A, Takeda K, et al. Targeted disruption of the Chop gene delays endoplasmic reticulum stress-mediated diabetes. J Clin Invest 2002;109:525–532
23. Zinszner H, Kuroda M, Wang X, et al. CHOP is implicated in programmed cell death in response to impaired function of the endoplasmic reticulum. Genes Dev 1998;12:982–995
24. Izumi T, Yokota-Hashimoto H, Zhao S, Wang J, Halban PA, Takeuchi T. Dominant negative pathogenesis by mutant proinsulin in the Akita diabetic mouse. Diabetes 2003;52:409–416
25. Leiter EH. The genetics of diabetes susceptibility in mice. FASEB J 1989;3:2231–2241
26. Liu S, Mauvais-Jarvis F. Minireview: Estrogenic protection of beta-cell failure in metabolic diseases. Endocrinology 2010;151:859–864
27. Schuit FC, In't Veld PA, Pipeleers DG. Glucose stimulates proinsulin biosynthesis by a dose-dependent recruitment of pancreatic beta cells. Proc Natl Acad Sci USA 1988;85:3865–3869
28. Kiekens R, In 't Veld P, Mahler T, Schuit F, Van De Winkel M, Pipeleers D. Differences in glucose recognition by individual rat pancreatic B cells are associated with intercellular differences in glucose-induced biosynthetic activity. J Clin Invest 1992;89:117–125
29. Pipeleers D, Kiekens R, Ling Z, Wilikens A, Schuit F. Physiologic relevance of heterogeneity in the pancreatic beta-cell population. Diabetologia 1994;37(Suppl. 2):S57–S64
30. Trajkovski M, Mziaut H, Schubert S, Kalaidzidis Y, Altkrüger A, Solimena M. Regulation of insulin granule turnover in pancreatic beta-cells by cleaved ICA512. J Biol Chem 2008;283:33719–33729
31. Ling Z, Chen MC, Smismans A, et al. Intercellular differences in interleukin 1beta-induced suppression of insulin synthesis and stimulation of non-insulin protein synthesis by rat pancreatic beta-cells. Endocrinology 1998;139:1540–1545
32. Yusta B, Baggio LL, Estall JL, et al. GLP-1 receptor activation improves beta cell function and survival following induction of endoplasmic reticulum stress. Cell Metab 2006;4:391–406